OPTIMIZED THRESHOLD MONITORING

Tormod Kværna, Lyla Taylor, Frode Ringdal and Johannes Schweitzer, NORSAR

Sponsored by U. S. Department of Defense
Defense Threat Reduction Agency
Contract No. DSWA01-97-C-0128

ABSTRACT

We have continued our efforts to develop a fully automated tool for continuous threshold monitoring of a given target area. Several case studies have been conducted for the Indian, Pakistani, and Novaya Zemlya (NZ) test sites. Specifically, we have demonstrated the benefit of including the large aperture NORSAR array (NOA) for optimized threshold monitoring. After introducing so-called time delay corrections in the beam forming process, most of the beam signal amplitude is retained. However, the main benefit of including the NORSAR array is its excellent ability to suppress signals from events located outside the target area. Because of the large array aperture of about 60 km, the array response has a very narrow main lobe and relatively small side lobes.

Signals from events located outside the target area often cause a temporary degradation of the monitoring capability, resulting in peaks in the network threshold trace. Our approach is that if we are able to confidently associate these short-duration peaks with events located *outside* the target area, it is highly unlikely that an event simultaneously took place *within* the target area.

The first step in an automatic analysis of the threshold traces is to identify significant threshold peaks. In order to accommodate both undulations in the long-term background noise level and noise variability, we have developed a peak detection method based on estimates of the noise variance and the long-term trend of the threshold trace. For the NZ test site, the peak detection threshold is typically around m_b 2.0. Secondly, we have developed a procedure for association of network threshold peaks with arrivals detected at each individual station. If we can confidently state that these arrivals originated outside the target area, the corresponding threshold peak can be discarded from further consideration.

For arrivals detected at array stations, the estimated azimuth and apparent velocity can effectively be used as criteria for sorting out arrivals originating outside the target area. An additional criterion for sorting out non-critical arrivals is a confident association with an event located outside the target area. Such phase associations are currently available in the PIDC Reviewed Event Bulletin (REB) and the NORSAR automatic regional bulletin based on the Generalized Beam Forming algorithm.

Key Words: data processing and analysis

OBJECTIVE

The objective of this work has been to improve the Threshold Monitoring (TM) algorithm for use in monitoring compliance with the Comprehensive Test Ban Treaty. In particular, we have investigated improvements associated with the use of optimized bandpass filters, station-specific travel-time and slowness/azimuth corrections for sites to be monitored. Through integration of the TM results with traditional detector and event information we have further extended the automatic monitoring utility of the TM method.

RESEARCH ACCOMPLISHED

Seismic events occurring at or near the former underground nuclear test site on Novaya Zemlya have been subjected to extensive investigation over the last four decades, as monitoring of the events in this region has been of special interest to the international community. Following the developments of sensitive regional arrays in northern Europe (see **Fig. 1**), events with magnitudes as low as 2.5 have been successfully detected and located in this region.

The development of the Threshold Monitoring (TM) method (Kværna and Ringdal, 1999; Ringdal and Kværna, 1989, 1992) has further improved the monitoring capability of this area. By optimizing the processing parameters from recordings of previous events in the region, the joint TM processing of the regional arrays ARCES, SPITS, FINES, and NORES place an upper bound on possible events in this area, which during normal noise conditions fluctuates around magnitude 2.0. A typical example is shown in **Fig. 2,** where the upper trace shows the combined magnitude threshold for the four arrays processed. There are, however, often instances when the monitoring threshold is temporarily increased because of signals from events located outside the region of interest. For complete monitoring, we have until recently manually investigated the cause of these threshold peaks. The procedure used has been to compare the time intervals of the short duration threshold peaks to event and signal detection information found in standard event bulletins or signal detection lists. If a threshold peak could confidently be associated with an event located outside the target area, we considered it highly unlikely that another event simultaneously took place within the target area.

The current research has focused on the development of a fully automatic peak explanation facility for analysis of the magnitude threshold traces. In this way we intend to minimize the need for manual classification of the threshold peaks such that manual analysis will only be necessary when events within the actual target region occur. Although the focus of this paper is the Novaya Zemlya test site, the method will be directly applicable to any geographical areas like the other underground nuclear test sites.

Automatic detection of peaks in the network threshold trace

The first step in the automatic analysis of threshold traces is to identify significant threshold peaks. Our approach has been to develop a peak detection method based on estimates of the noise variance and the long term trend of the threshold trace. From experiments with various data sets, we have developed a method which comprises the following steps:

- Calculate the long-term-median (LTM) of the threshold trace with a typical window length of 30 minutes and a sampling interval of 5 minutes.
- Calculate the overall standard deviation (SIGMA) of the threshold trace around the long-term-median after removing the upper 10% of the data values. The removal of the upper 10% of the data values is done to reduce the influence of the threshold peaks on the estimate of the standard deviation.
- Define the peak detection limit as LTM + 5 * SIGMA
- Alternatively, the peak detection limit is defined separately for each threshold trace using a predefined shift above the LTM. For the Novaya Zemlya network threshold trace we have initially found that LTM + 0.35 provides a reasonable peak detection limit, whereas the individual station/phase threshold traces show a somewhat larger variability, and LTM + 0.4 was consequently used.

Fig. 3 shows a panel with threshold traces for 18 May 1999 with predefined peak detection limits superimposed. Notice that six peaks are identified on the network threshold trace which we have to investigate in more detail.

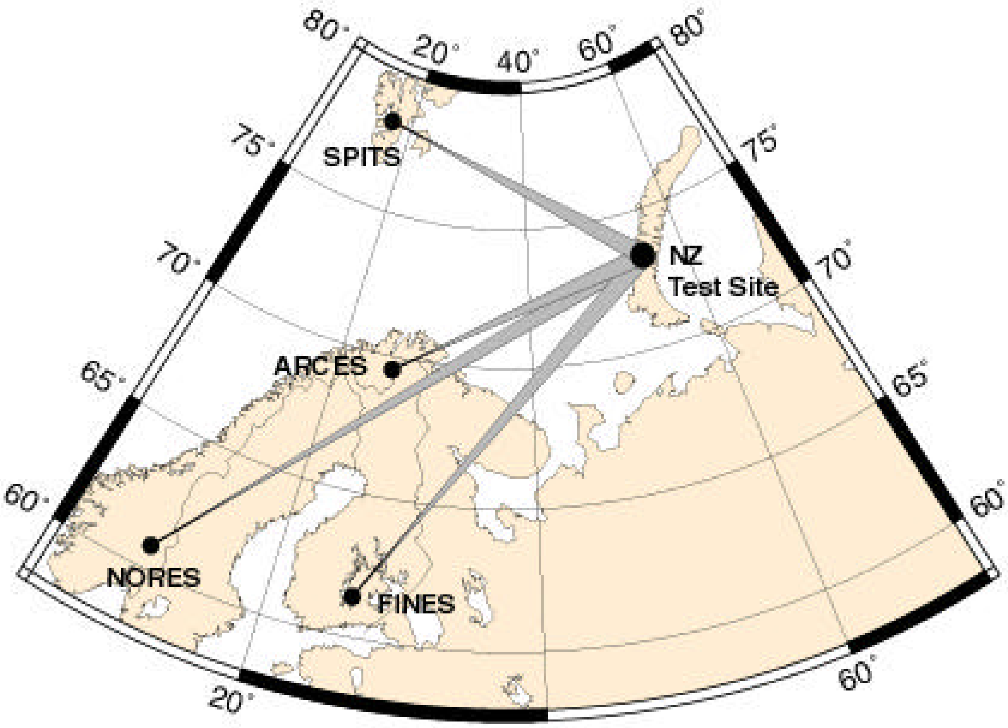

Fig. 1. Map of Novaya Zemlya and the locations of the four arrays (SPITS, ARCES, FINES, and NORES) used to monitor the region around the former underground nuclear test site.

Association of network threshold peaks with signals detected at each individual array

In order to relate the peaks of the network threshold trace to information obtained by traditional signal processing at each array, we first have to determine the time intervals associated with each network threshold peak. Through experiments, the following procedure has been established:

- Detect peaks on the threshold traces calculated for each individual phase. Examples are given in the lower panels of **Fig. 3**.
- For each phase considered, find the peak detection intervals overlapping the peak detection intervals of the network threshold trace, and use the union as the time interval of interest. See **Fig. 4** for details.
- The x-axes of the threshold traces show origin times at the NZ test site. When searching the detection lists for signals associated with the threshold peaks, we have to shift the detection times in accordance with the expected phase travel time from the NZ test site to the actual array.
- From statistics on the distribution of slowness and azimuth estimates, we define for each phase a critical azimuth and slowness range for events in the vicinity of the NZ test site. The numbers used are given in **Table 1**. Detected signals with azimuth and slowness estimates falling outside the critical ranges are assumed to be caused by events located outside the NZ testing area, otherwise, further offline analysis will be required to determine the cause of the threshold peak. Examples of array signal detections associated with the network threshold peaks are shown in **Fig. 5** and **Fig. 6**.

- An overview of the results after associating the network threshold peaks with signals detected at each individual array is given in **Fig. 3**. For each of the P-phase threshold traces we have only considered threshold peaks associated with a network threshold peak. In the four lower panels, an arrow indicates that we have found one or more signal detections with azimuth and slowness estimates within the critical ranges.
  For the peaks of the network threshold trace shown on top of the figure, an arrow indicates that at least one of the arrays has a detection with azimuth and slowness estimates within the critical ranges. The causes of these threshold peaks have to be investigated in more detail, e.g. by comparing to existing event bulletins or by offline analysis of the raw seismic data.
- In order to investigate the threshold peaks having phase observations with slownesses and azimuths typical for NZ events, we have introduced the functionality of comparing the critical signals to phases associated to events reported in the NORSAR bulletin of events in northern Europe (Kværna et al., 1999). The critical threshold peak at 20:20 on 18 May 1999 (see **Fig. 3**) is in this way found to be caused by an m_b 4.5 event located north of Severnaya Zemlya. For this location, P-phases observed at FINES and NORES have azimuths and slownesses comparable with P-phases from events at the NZ test site. Detailed information on the critical detections is given in **Table 2**.

There will still be a few situations when we have threshold peaks that cannot be explained by the procedures outlined above. In such situations we have to carry out additional manual analysis to determine the cause of the event. Typical situations may be signal detections in the coda of larger teleseismic events.

Array	Phase	Expected Azimuth (degrees)	Lower Azimuth (degrees)	Higher Azimuth (degrees)	Expected Slowness (sec/deg)	Lower Slowness (sec/deg)	Higher Slowness (sec/deg)
ARCES	P	62.2	47.2	77.2	11.22	10.59	17.11
ARCES	S	64.3	49.3	79.3	23.21	19.86	31.77
SPITS	P	97.6	77.6	117.6	13.24	10.59	19.86
SPITS	S	97.6	77.6	117.6	23.16	19.86	34.75
FINES	P	29.6	11.6	47.6	11.63	10.59	14.83
NORES	P	33.6	18.6	48.6	10.85	9.27	14.26

Table 1: Definition of critical azimuth and slowness ranges for phases from events near the NZ test site

CONCLUSIONS AND RECOMMENDATIONS

Concerning optimized site-specific threshold monitoring it is important to be aware that the main purpose of the method is to call attention to any time instance when a given threshold is exceeded. Through the development of the automatic explanation function for threshold peaks we have further reduced the need for manual analysis. This will enable analysts to focus their efforts on those events that are truly of interest in a continuous monitoring situation.

Through the integration of threshold monitoring with the results provided in traditional detection lists and event bulletins we have further improved the automatic monitoring capability of a given target area. For the Novaya Zemlya test site the monitoring threshold fluctuates around magnitude 2.0 during normal noise conditions, and we plan to evaluate the procedure in more detail by accumulating processing statistics for a longer time interval.

For the primary seismic stations of the International Monitoring System (IMS) for verifying compliance with the CTBT, we have available optimized processing parameters for the Indian and Pakistani test sites, and we plan to derive processing parameters for the former Chinese, French, and US test sites. There is, however, a need to further investigate the integration of three-component stations into the automatic explanation facility for threshold peaks.

Configuration	**Edge 1**	**Edge 2**	**Duration (sec)**	**Max. mag.**
Network	1999-138:20.21.28	1999-138:20.28.23	416	2.87
FINES P	1999-138:20.22.09	1999-138:20.28.16	367	3.78
NORES P	1999-138:20.21.27	1999-138:20.22.53	87	3.74

Station Phase	Arid	Arrival time (Origin time)	SNR	App. Vel. (km/s)	Azim. (deg)	R.pwr.	dS (s/deg)
FINES P	91336	1999-138:20.25.56.125 *(1999-138:20.22.11.925)*	45.1	10.3	12.7	0.98	3.40
FINES P	91339	1999-138:20.26.13.800 (*1999-138:20.22.29.600)*	2.9	8.7	15.9	0.97	3.13
NORES P	91473	1999-138:20.26.27.393 (*1999-138:20.21.45.993)*	3.0	11.6	23.3	0.93	2.22

Table 2: Definition of the critical threshold peaks shown in Fig. 3. The phases with critical slownesses and azimuths are given in the lower part of the table. These phases are all associated with a magnitude 4.5 event located north of Severnaya Zemlya

REFERENCES

Kværna, T. and F. Ringdal (1999): Seismic Threshold Monitoring for Continuous Assessment of Global Detection Capability, accepted for publication in BSSA.

Kværna, T., J. Schweitzer, L. Taylor and F. Ringdal (1999): Monitoring of the European Arctic using regional generalized beamforming. In: *NORSAR Semiannual Tech. Summ. 1 October 1998 - 31 March 1999, NORSAR Sci. Rep. 2-98/99*, Kjeller, Norway

Ringdal, F. & T. Kværna (1989): A multichannel processing approach to real time network detection, phase association and threshold monitoring, *Bull. Seism. Soc. Am.*, 79, 1927-1940.

Ringdal, F. & T. Kværna (1992): Continuous seismic threshold monitoring, *Geophys. J. Int.*, 111, 505-514.

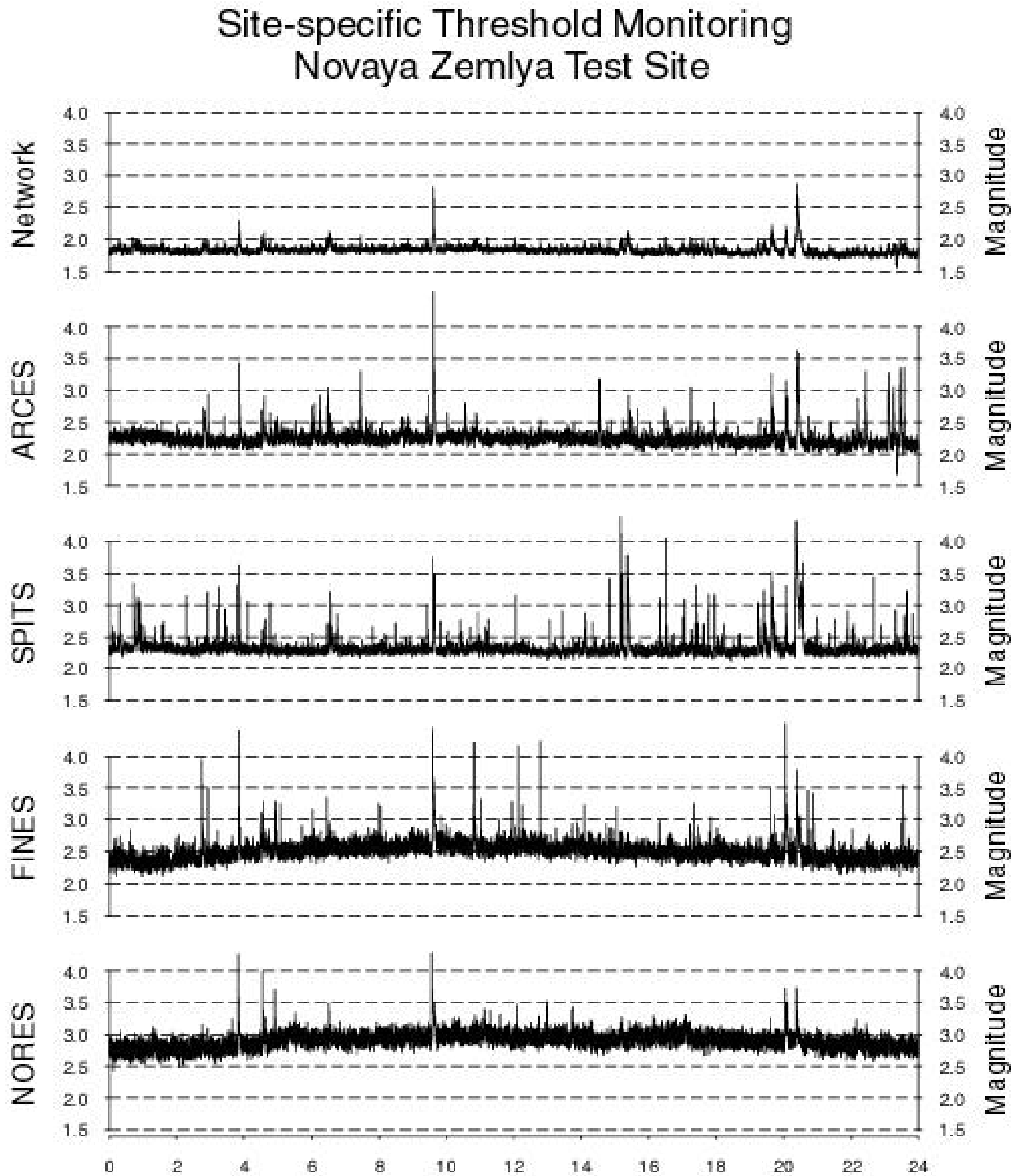

Fig. 2. Results from threshold monitoring of the Novaya Zemlya Test Site for 18 May 1999. The network trace on top is the combined threshold trace, using P phases for all arrays and in addition S phases for ARCES and SPITS. The traces for each of the four stations (P phases only) are shown below the network trace.

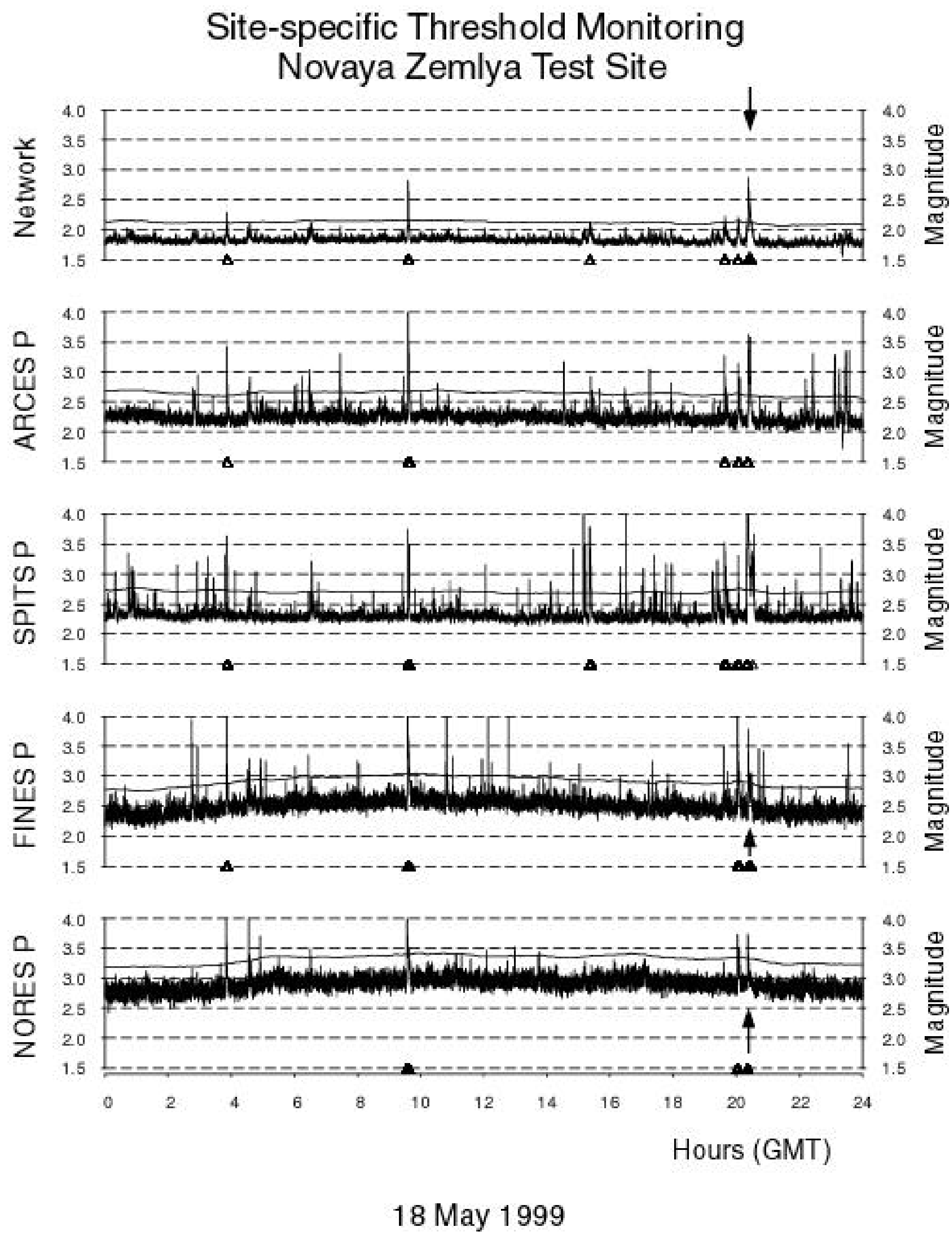

Fig. 3. Results from threshold monitoring of the Novaya Zemlya Test Site for 18 May 1999 with pre-defined peak detection limits superimposed. For each of the P-phase threshold traces we have only considered threshold peaks associated with a <u>network</u> threshold peak. In the four lower panels, an arrow indicates that we have found <u>one or more</u> signal detections with azimuth and slowness estimates within the critical ranges.

For the peaks of the network threshold trace shown on top of the figure, an arrow indicates that at least one of the arrays has a detection with azimuth and slowness estimates within the critical

ranges. The network threshold peak around 20:20, marked by the arrow, is caused by an mb 4.5 event located north of Severnaya Zemlya.

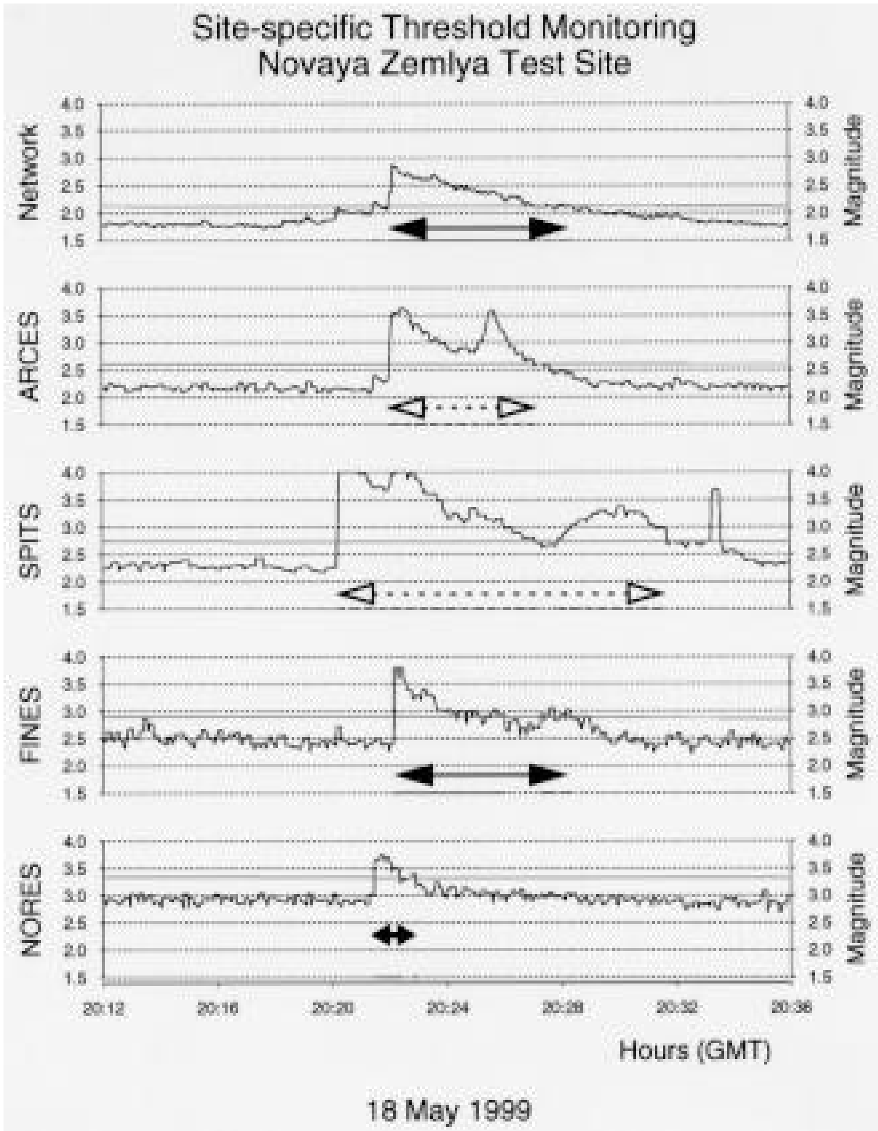

Fig. 4. Illustration of the procedure for defining the time intervals used for finding matching detections. For each phase considered, we find the peak detection intervals overlapping the peak detection intervals of the network threshold trace, and use the <u>union</u> as the searching time interval for each station. When searching the detection lists for signals associated with the threshold peaks, we have to shift the detection times in accordance with the expected phase travel time from the NZ test site to the actual array.

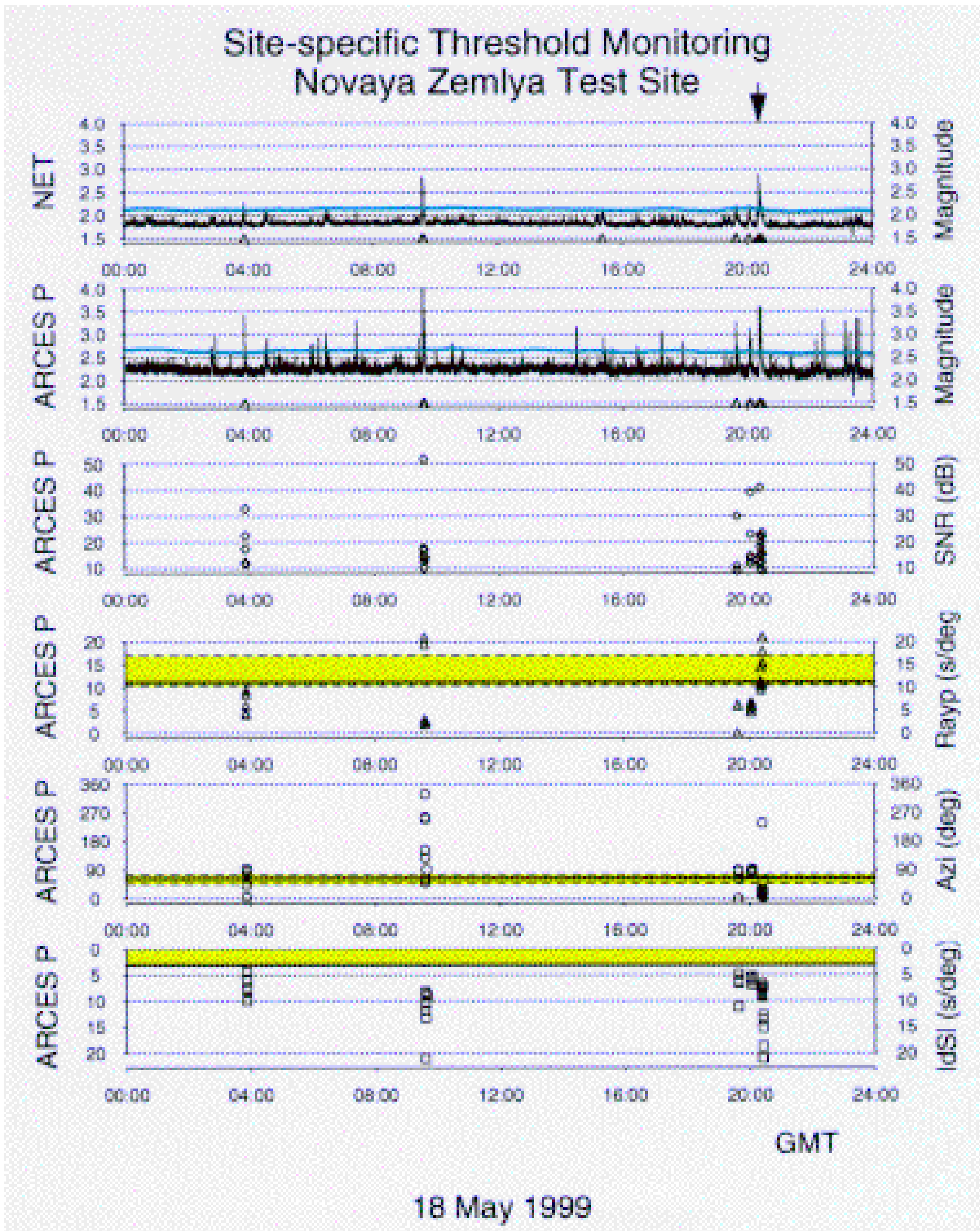

Fig. 5. Results from correlating peaks of the NZ magnitude thresholds with information from the signal detector at ARCES. The two upper panels show the threshold traces for the network and for the ARCES P-phase. The peak detection limits are superimposed. Information about the signal detections associated with the network threshold peaks is displayed in the four lower panels. The critical ranges of slowness (ray parameter) and azimuth are shaded grey in panels 4 and 5, and the bold dashed lines indicate the expected values of P-phases from the NZ test site. The panel at the bot-

tom indicates the differences in horizontal slowness estimates between the detected signals and the expected value for P-phases from the NZ test site (in s/deg). The shaded region within 3 s/deg indicates the approximate range of interest for NZ P-phases. Signals satisfying both the azimuth and slowness criteria are shown by filled symbols. Notice that no ARCES detections satisfies both the azimuth and slowness criteria.

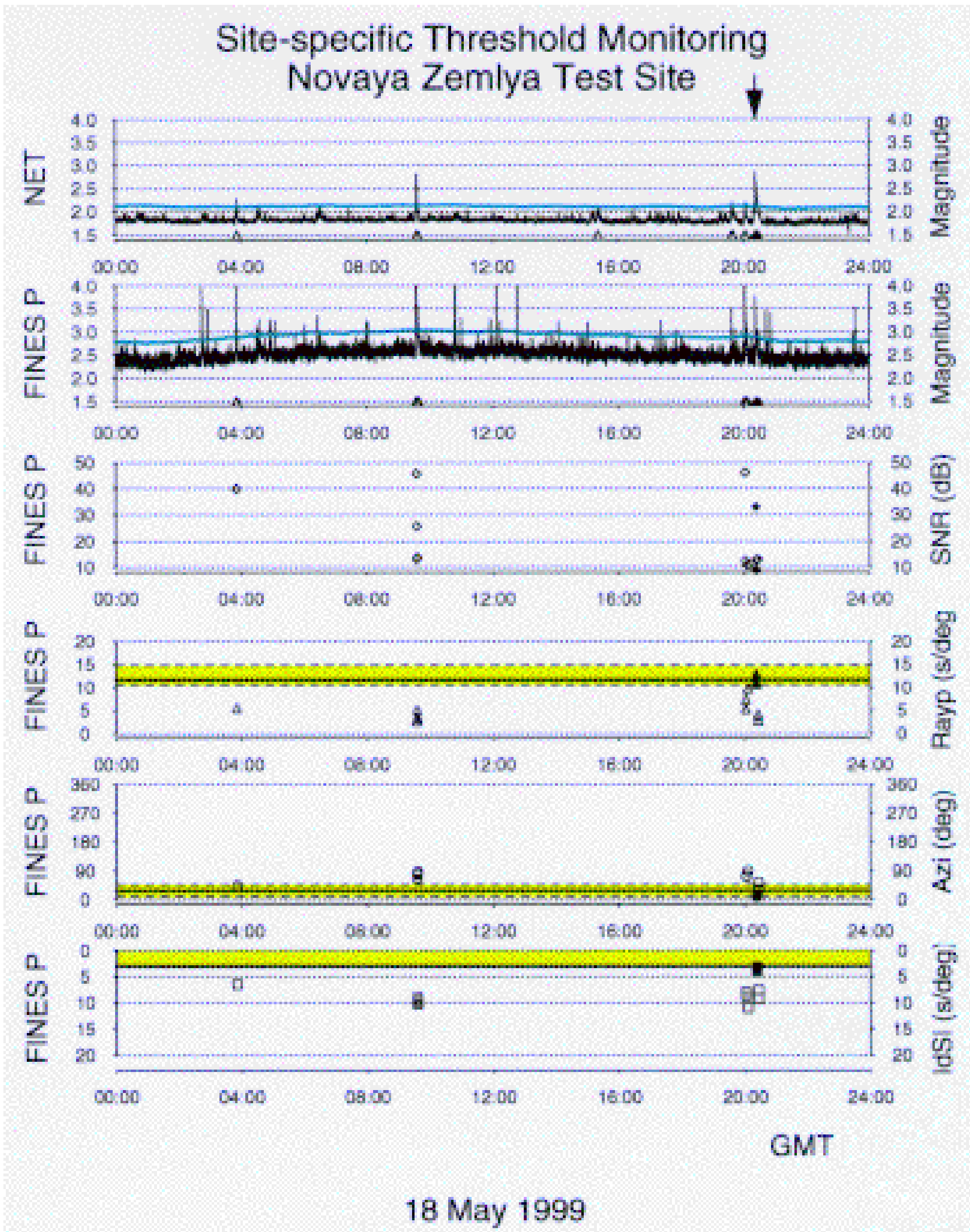

Fig. 6. Results from correlating peaks of the NZ magnitude thresholds with information from the signal detector at FINES. A detailed explanation of the figure content is given in the caption of Fig. 5. Notice that for the network threshold peak around 8:20 p.m. there are two FINES detections with azimuth and slowness estimates that fall within the critical range for P-phases from NZ events. This is because the event location near Severnaya Zemlya is at about the same azimuth from

FINES as NZ, and with a similar expected phase velocity. However, when combined with other stations (e.g. ARCES, see Fig. 5), it becomes clear that the signal cannot be from the NZ test site